Rab8, a Small GTPase Involved in Vesicular Traffic between the TGN and the Basolateral Plasma Membrane

Lukas A. Huber, Sanjay Pimplikar, Robert G. Parton, Hilkka Virta, Marino Zerial, and Kai Simons

Cell Biology Programme, European Molecular Biology Laboratory, Postfach 10.2209, D-69012 Heidelberg, Germany

Abstract. Small GTP-binding proteins of the rab family have been implicated as regulators of membrane traffic along the biosynthetic and endocytic pathways in eukaryotic cells. We have investigated the localization and function of rab8, closely related to the yeast YPT1/SEC4 gene products. Confocal immunofluorescence microscopy and immunoelectron microscopy on filter-grown MDCK cells demonstrated that, rab8 was localized to the Golgi region, vesicular structures, and to the basolateral plasma membrane. Two-dimensional gel electrophoresis showed that rab8p was highly enriched in immuno-isolated basolateral vesicles carrying vesicular stomatitis virus-glycoprotein (VSV-G) but was absent from vesicles transporting the hemagglutinin protein (HA) of influenza virus to the apical cell surface.

Using a cytosol dependent in vitro transport assay in permeabilized MDCK cells we studied the functional role of rab8 in biosynthetic membrane traffic. Transport of VSV-G from the TGN to the basolateral plasma membrane was found to be significantly inhibited by a peptide derived from the hypervariable COOH-terminal region of rab8, while transport of the influenza HA from the TGN to the apical surface and ER to Golgi transport were unaffected.

We conclude that rab8 plays a role in membrane traffic from the TGN to the basolateral plasma membrane in MDCK cells.

RECENT studies have demonstrated the involvement of small GTP-binding proteins, homologous to the protooncogene ras, in the regulation of membrane traffic (for reviews see Balch, 1990; Hall, 1991; Olkkonen et al., 1993). The first two to be characterized were yptlp and sec4p in *Saccharomyces cerevisiae* (Gallwitz et al., 1983; Segev et al., 1988; Salminen and Novick, 1987). The mammalian homologues of these proteins, are called rab proteins, and form a large family of at least 30 members (Zahraoui et al., 1989; Touchot et al., 1987; Chavrier et al., 1990*b*). Presently the field is one of expansion; new members of the families are being identified (Zahraoui et al., 1989; Touchot et al., 1987; Chardin and Tavitian, 1989; Bucci et al., 1988; Didsbury et al., 1989; Polakis et al., 1989; Sewell and Kahn, 1988; Chardin et al., 1988; Pizon et al., 1988; Zahraoui et al., 1988) and also a great number of associated proteins that affect the biochemical activity of small GTP-binding proteins have been reported (Burstein et al., 1991; Tan et al., 1991; Shimizu et al., 1991; Sasaki et al., 1991). Morphological and biochemical studies have indicated that these proteins are localized to different segments of the biosynthetic (Mizoguchi et al., 1989; Goud et al., 1990; Chavrier et al., 1990*a*; Darchen et al., 1990; Plutner et al., 1990; Fischer von Mollard et al., 1991) and endocytic (Bucci et al., 1992; Chavrier et al., 1990*a*; Van der Sluijs et al., 1991, 1992; Lombardi et al., 1993) pathways where they seem to regulate distinct steps of vesicular transport. Proteins of the ypt1/sec4/rab subfamily are thought to be involved in conferring specificity to targeting or fusion of transport vesicles with their correct acceptor compartment (Bourne, 1988; Pfeffer, 1992). Sar/ARF constitute another family of small GTP-binding proteins. Sar1p is required for budding of vesicles from the ER in vitro (Oka et al., 1991). ADP-ribosylation factor (ARF)[1] is highly enriched in Golgi-derived vesicles and was postulated to be involved in the budding and uncoating of these vesicles (Serafini et al., 1991). Recently a role for ARF proteins in trafficking in the biosynthetic and endocytic pathways has also been reported (Koch et al., 1992; Kahn et al., 1992; Lenhard et al., 1992). With the long-term goal of elucidating the mechanisms responsible for membrane traffic in polarized epithelia, we have been searching for rab proteins involved in apical and basolateral trafficking in polarized epithelial cells. MDCK cells are a well-established model for studying the development and maintenance of cell surface polarity. Apical and basolateral plasma membrane proteins in MDCK cells are sorted in the TGN by inclusion into separate carrier vesicles that transport the proteins to the correct destination (Griffiths and Simons, 1986; Hughson et al., 1988). Chavrier et al. (1990*b*) screened a MDCK cell cDNA library with a degenerate oligonucleotide corresponding to a conserved sequence shared by all GTP-binding proteins of the Ypt1/Sec4 subfamily. 11

1. *Abbreviations used in this paper:* ARF, ADP-ribosylation factor; IEF, isoelectric focusing; PCR, polymerase chain reaction; PNS, postnuclear supernatant; SLO, streptolysin; 2D, two dimensional.

clones encoding putative GTP binding proteins were isolated. Rab8 was one of the GTP-binding proteins that came up in the first round of screening. Rab8 is highly related to the yeast proteins yptlp and sec4p. The overall sequence identity in the region excluding the variable NH_2 and COOH termini is around 60%. Most importantly the sequence identity is strikingly high in the effector domain. While a mammalian homolog of yptlp has been identified (rabl) and shown to replace the yptlp functionally in *S. cerevisiae*, a mammalian counterpart of sec4p has not yet been identified. Rab8p is a candidate for post-Golgi transport functions.

In this study we have used specific antibodies against rab8p to investigate its cellular localization. In addition, immuno-isolated apical and basolateral transport vesicles were analyzed for their content of GTP-binding proteins using high-resolution two-dimensional (2D) gel electrophoresis. Finally, recently established transport assays in permeabilized cells were used (Kobayashi et al., 1992; Pimplikar and Simons, 1993) to study the involvement of rab8p in biosynthetic traffic in MDCK cells. All together the results demonstrate that rab8p is involved in regulating transport from the TGN to the basolateral cell surface.

Material and Methods

Cell Culture

Media and reagents for cell culture were purchased from Gibco Biocult (Eggenheim, Germany) and Biochrom (Berlin, Germany). Growth medium for MDCK strain II cells consisted of MEM with Earle's salts (E-MEM) supplemented with 10 mM Hepes, pH 7.3, 10% FCS, 100 U/ml penicillin, and 100 μg/ml streptomycin. MDCKII cells were grown and passaged as described previously (Matlin et al., 1981). BHK 21 cells were grown in Glasgow's modified Eagle's medium, supplemented with 5% FCS, 2 mM glutamine, 100 U/ml penicillin, 100 μg/ml streptomycin, and 10% tryptosephosphate at 37°C in 5% CO_2. NIH3T3 and HeLa cells were grown in D-MEM (1 g/liter glucose) supplemented with 5% FCS, 2 mM glutamine, 100 U/ml penicillin, and 100 μg/ml streptomycin. Infection medium was composed of E-MEM supplemented with 10 mM Hepes, pH 7.3, 0.2% BSA, 100 U/ml penicillin, and 100 μg/ml streptomycin. For large scale isolation of vesicles cells from a 75 cm^2 flask were seeded on a single 100-mm diam, 0.4-μm pore size Transwell filter as described previously (Wandinger-Ness et al., 1990). For in vitro transport assays and immunofluorescence/immunoelectron microscopy, 2.4 million cells were seeded on 24 mm Transwell filters.

Plasmid Construction

Full-length cDNAs of rab proteins expressed and studied here were inserted into pGEM1 under the control of the T7 promotor according to the previously described procedure for transient expression of rab proteins with the T7 RNA polymerase-recombinant vaccinia virus system (Chavrier et al., 1990*b*). To express the rab8 protein in vivo we inserted the rab8 cDNA under the control of a T7 promoter. First, we constructed plasmid pBSSK-rab8 containing the complete coding sequence of rab8. This plasmid was derived by re-engineering pBSSK-2, which was obtained by in vivo excision of the λ UNI-ZAP XR phage vector (Chavrier et al., 1990*b*) and lacked the segment encoding the first 46 NH_2-terminal amino acid residues of rab8. The fragment encoding this region was generated using the polymerase chain reaction (PCR) from MDCK oligo$(dT)_{12-18}$-primed cDNA using the oligonucleotides 5'AGTCGGATCCATATGGCGAAGACCTACGATTACCTG3' and 5'TTGATTCCATAGTCCAGGGCC3' as primers. After restriction with BamHI and PstI, the PCR product was inserted into pBSSK-2 cut with the same enzymes in order to restore the full-length coding region of rab8. The vector region containing the PCR amplified DNA was sequenced by the dideoxy method to rule out the presence of mutations. The sequence obtained perfectly matched that of the rab8 cDNA described in Chavrier et al. (1990*b*).

Plasmid pGEM1-rab8 was constructed by inserting a ~2-kb BamHI–XhoI DNA fragment, containing the whole rab8 cDNA isolated from pBSSK-rab8, into pGEM1 restricted with BamHI and SalI. The construct was checked by restriction endonuclease digestion and in vitro transcription–translation analysis.

T7 RNA Polymerase Recombinant Vaccinia Virus Infection and Transfection

MDCK strain II cells were split 24–36 h before transfection so that on the day of transfection they were ~80% confluent. The cells were washed twice with PBS and trypsinized (1× Trypsin-EDTA solution; Gibco Biocult) before infection. Cells were then washed twice in serum-free medium and resuspended. Infection with T7 polymerase-recombinant vaccinia virus (Fuerst et al., 1986) was carried out in serum-free medium in solution with 3–5 pfu/cell at room temperature for 30 min with intermittent agitation. After 30 min cells were plated to dishes again, and after serum supplementation (5%), transfected using DOTAP reagent (Boehringer Mannheim, Mannheim, Germany) according to the manufacturer's instructions, which allows transfection in serum-supplemented medium conditions. Cells were then incubated in the presence of 10 mM hydroxyurea for 5 h at 37°C in 5% CO_2 and processed for further analysis.

Two-dimensional Gel Electrophoresis

A combination of isoelectric focusing (IEF) and SDS-PAGE was used to resolve proteins in two dimensions essentially as described previously (Bravo, 1984; Celis et al., 1990). For IEF samples were solubilized in 9.8 M urea, 4% (wt/vol) NP-40, 2% (vol/vol) ampholines, pH 7–9 (Pharmacia LKB, Bromma, Sweden), and 100 mM DTT. Tube gels used for the first dimension were 25-cm long and had an internal diameter of 2.5 mm. IEF gels were run at 1,200 V for 17 h. The pH gradient after electrophoresis ranged from 4.57 to 8.03 and was linear between pH 4.6–7.2 (Wandinger-Ness et al., 1990). For the second dimension 15% SDS-PAGE (15% wt/vol acrylamide, 0.075% wt/vol *N,N'*-methylene-bisacrylamide; stacking gels were 5% wt/vol acrylamide, 0.25% wt/vol *N,N'*-methylene-bisacrylamide) was used.

Transfer to Nitrocellulose Blots and [α^{32}P] GTP Overlay

For transfer to nitrocellulose and GTP overlay we have modified a protocol based on the method from Lapetina and Reep (Lapetina and Reep, 1987). Proteins (60–70-μg total) were separated by high-resolution two-dimensional gel electrophoresis as described above, washed 2 × 15 min in 50 mM Tris-HCl, pH 7.5/20% glycerol, and electrophoretically transferred to nitrocellulose paper in 10 mM $NaHCO_3$/3 mMNa_2CO_3 (pH 9.8). The transfer blots were rinsed for 30 min in GTP-binding buffer (50 mM NaH_2PO_4, pH 7.5, 10 μM $MgCl_2$, 2 mM DTT, 0.2% Tween 20, and 4 μM ATP as competing substrate), and then incubated with [α^{32}P] GTP (1 μCi/ml, sp act 2,903 Ci/mmol, 1 Ci=37 GBq) for 2 h. The blots were rinsed for 60 min with several changes of binding buffer and air dried. [α^{32}P] GTP binding was visualized by autoradiography (12–24 h, −80°C) using Kodak Xomat Ar film with an intensifying screen (Eastman Kodak Co., Rochester, NY). Molecular masses were determined by comparison to prestained SDS/PAGE molecular weight standards (Bio-Rad Labs, Richmond, CA) electrophoresed in the gels and transferred to nitrocellulose blots.

Preparation of Total Cellular Membrane Fractions

A postnuclear supernatant (PNS) was prepared as described previously (Kurzchalia et al., 1992; Gorvel et al., 1991), transferred to a TLA100.2 microfuge tube and centrifuged for 30 min, 4°C at 60,000 rpm. The supernatant (cytosol fraction) and the pellet were separated and taken up in IEF sample buffer and processed for high-resolution 2D gel analysis.

Immunoblotting

For Western blots, protein samples were lysed in standard SDS sample buffer and extracts were electrophoresed on 10% polyacrylamide gels. Separated proteins were transferred onto nitrocellulose filters. Filters were prewashed in PBS/4% milk, 0.2% Tween 20, and 0.1% sodium azide for 2 h at room temperature. After three washes of 10 min in PBS/0.2% Tween 20, the filters were incubated for 1 h with primary antibodies diluted in PBS/4% milk, 0.2% Tween 20, and 0.1% sodium azide. After extensive

washing filters were incubated with a HRP-labeled secondary antibody (Bio-Rad Labs) for 1 h, washed, and developed.

Viral Infection

Influenza WSN ts61 and vesicular stomatitis virus (VSV) stocks were prepared according to Bennett et al. (1988) and Hughson et al. (1988), respectively. Infections were performed by rinsing cells growing on 100 mm filters with infection medium and transferring the filters back to the original 10 cm dishes. The virus stocks were diluted in infection medium and added in a volume of 500 μl to the apical side of the filters (Wandinger-Ness et al., 1990) at a multiplicity of 5 pfu/cell (WSN ts61) or 50 pfu/cell (VSV). After adsorption to the cells for 1 h at 31°C for WSN ts61, or 37°C for VSV, the viral inoculates were aspirated and fresh infection medium was added to the apical and basolateral side. Infections were continued for an additional 3.5 h at 39°C (WSN ts61) or 2.5 h at 37°C (VSV). To incubate cells for 2 h in a waterbath at 20°C, the medium was replaced with Hepes-buffered, low bicarbonate medium.

Vesicle Isolation from Perforated Cells and Immunoisolation

After the 20°C block filter-grown cultures were perforated (Bennett et al., 1988) and post-TGN-derived vesicles were collected and concentrated as described (Wandinger-Ness et al., 1990).

Immuno-isolation of these vesicle fractions after viral infection was carried out as described previously (Wandinger-Ness et al., 1990). Briefly, for each immunoisolation a gradient-purified vesicle fraction from one 100 mm filter was used. Aliquots were incubated with either specific or control antibodies and immunoabsorbed with cellulose fibers as described (Wandinger-Ness et al., 1990). Mouse mAbs directed against the cytoplasmic domains of VSV-G protein (Kreis, 1986) and influenza PR8 (Hughson et al., 1988) were used in the form of concentrated hybridoma culture supernatants. After collection the fibers were washed and pelleted as described (Wandinger-Ness et al., 1990) and the pellet was resuspended directly in 50 μl IEF sample buffer and processed for 2D gel analysis and GTP overlay.

rab8 Peptides

The peptide was derived from the COOH-terminal hypervariable region of rab8. This region differs among the different rab proteins. The peptide sequence was KAKMDKKLEGNSPQGSNQGVK (position 170-190), beginning from the last amino acid residue of α helix 5 as deduced from the structure of ras p21, and excluding the cysteine motif. This peptide was either used for raising and purifying specific antibodies against rab8 or for in vitro transport assays in permeabilized MDCK cells.

Preparation of Antiserum against rab8

Polyclonal antibodies were raised against synthetic peptides covalently coupled to keyhole limpet hemocyanin (Calbiochem-Norabiochem, LaJolla, CA) (Kreis, 1986). Affinity purification was carried out over a matrix of peptide coupled to Sepharose 4B. Immobilization of the peptide to cyanogen-bromide-activated Sepharose 4B (Pharmacia, Upsala, Sweden) was performed in coupling buffer (0.1 M $NaHCO_3$, pH 8.5, 0.5 M NaCl) at 4°C. Specific antibodies were bound overnight at 4°C on the peptide column and eluted in 0.2 M glycine-HCl (pH 2.8) neutralized by the addition of 1 M Tris-HCl (pH 8.0). Affinity-purified antibodies were dialyzed against 50% PBS/glycerol (4°C, overnight) and stored at −20°C.

Immunofluorescence

Cells were grown on 11-mm-round glass coverslips for 24–48 h before treatment. Cells were washed once with PBS and permeabilized with 0.01% Saponin (Sigma, Deisenhofen, Germany) in 80 mM K-Pipes (pH 6.8), 5 mM EGTA, 1 mM $MgCl_2$ for 5 min. Cells were fixed with 3% paraformaldehyde in PBS (pH 7.4) for 15 min, free aldehyde groups were quenched with 50 mM NH_4Cl in PBS for 15 min. After fixation coverslip-grown cells were processed as described previously (Chavrier et al., 1990*a*), mounted in moviol and viewed with a Zeiss Axiophot Photomicroscope (Carl Zeiss, Oberkochen, Germany). Filter-grown MDCK strain II cells were also saponine extracted and further processed as described (Bacallao et al., 1989). Filters were mounted with spacers (nail polish drops) in 50% glycerol/PBS. They were then viewed with the EMBL confocal microscope and photographed on Kodak Tmax 100 film with a Polaroid Freeze frame directly from the monitor.

Immunoelectron Microscopy

Fully polarized, filter grown MDCKII cells were fixed with 8% paraformaldehyde in 250 mM Hepes (pH 7.35). Pieces of filter were sandwiched together with 10% gelatin in PBS, infiltrated with sucrose, and frozen in liquid nitrogen. After sectioning, grids were incubated for 1 h at 37°C on PBS to dissolve and remove the gelatin. Labeling with antibodies and protein A-gold was performed as described previously (Griffiths et al., 1984; Griffiths et al., 1985).

In Vitro Transport of VSV-G and HA in Permeabilized MDCKII Cells

MDCKII cells were grown on 24 mm Transwell filters for 3 d before being infected with VSV or influenza viruses. The cells were pulse labeled with [^{35}S] methionine for 6 min, chased for 6 min in the presence of methionine at 37°C with further incubation at 20°C for 60 min to block the viral glycoproteins in the TGN as described (Kobayashi et al., 1992; Pimplikar and Simons, 1993). The cells were then permeabilized with streptolysin O (SLO; a generous gift from Dr. S. Bhakdi, University of Mainz, Mainz, Germany) as described recently (Kobayashi et al., 1992; Pimplikar and Simons, 1993). The in vitro transport of HA and VSV was performed as described (Kobayashi et al., 1992; Pimplikar and Simons, 1993) in the presence or absence of exogenously added cytosol (HeLa cytosol, 8 mg/ml) that was preincubated with 10–100 μM peptide derived from the hypervariable COOH-terminal region of rab8p. The same peptide sequence was used as for the preparation of antiserum against rab8. The rab5ap peptide used here as control for the basolateral assay was derived from the NH_2-terminal region of rab5a. The peptide sequence was MANRGATRPNGPNTGNK, beginning from the first amino acid residue of rab5a.

All experiments were carried out with duplicate filters for each transport condition and the values expressed as means of the duplicates from four experiments. Samples were analyzed by SDS-PAGE, autoradiographed, scanned with a PhosphorImager (Molecular Dynamics GmbH, Krefeld, Germany) and the band intensities were calculated with ImageQuant software. The amount of HA transported to the apical surface was measured by its sensitivity to cleavage by trypsin and calculated as described before (Matlin and Simons, 1984) (% transport = 2 × HA2/HA0 + HA2 × 100). Cytosol-dependent transport is expressed as being 100%. The amount of VSV-G transported to the basolateral surface was detected by surface immunoprecipitation with an affinity-purified antibody directed against the luminal domain of VSV-G protein (Pfeiffer et al., 1985) and calculated as the amount of VSV-G bound to protein A-agarose resin. The values for VSV-G transport are expressed as cytosol dependent transport being 100% ([transport in the presence of cytosol] − [transport in the absence of added cytosol]). The values for ER to Golgi transport are expressed as a percentage of the aquired Endo H resistance (HA resistant/[HA resistant + HA sensitive]) of HA.

Results

Cellular Localization of rab8p by Immunofluorescence Microscopy

An affinity-purified anti-peptide antibody raised against the COOH-terminus of rab8p was used for cellular localization of rab8p. The specificity of the antibody was confirmed by immunoblot analysis using rab8 and rab10 proteins (Fig. 1) and peptide inhibition (10 μg/ml) in indirect immunofluorescence (results not shown). Rab8 and rab10 proteins were expressed in *E. coli* BL21(E3) using the pET3a expression system (Studier et al., 1990). The antibody reacted specifically with both rab8p expressed in *E. coli* (Fig. 1, lane *1*) and with the endogenous protein in MDCK cells (Fig. 1 , lanes *3* and *4*), whereas no specific signal was detected with rab10p (Fig. 1, lane *2*). As revealed by Western blot analysis only a small fraction of rab8p was recovered in the cytosol fraction (Fig. 1, lane *3*), whereas most of rab8p was found to be membrane associated (Fig. 1, lane *4*).

For immunofluorescence microscopy MDCKII, HeLa, BHK, and NIH3T3 cells were permeabilized with saponin

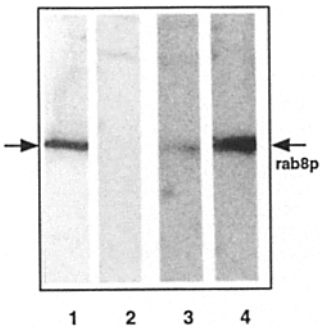

Figure. 1 Immunoblot analysis of total proteins from *E. coli* BL21(DE3) expressing rab8p (lane *1*) and rab10p (lane *2*, this protein migrates exactly with the same mobility as rab8p, see also Fig. 5) and of MDCK II cytosol (lane *3*) and crude membrane fractions (lane *4*). Proteins (~100 μg) were separated by 15% SDS-PAGE, electrophoretically transferred onto nitrocellulose filters, and incubated with affinity-purified anti-rab8p peptide antibodies. Bands were visualized using either an alkaline phosphatase conjugated goat anti-rabbit antibody (lanes *1* and *2*) or an HRP conjugated goat anti-rabbit antibody and an enhanced chemoluminescence (ECL) Western blotting system (lanes *3* and *4*).

and the cytoplasmic pool of GTP-binding proteins was extracted with K-Pipes buffer. After this extraction the antibodies detected rab8p associated with cellular membranes. In all cell types investigated (Fig. 2, *a–d*) the staining was found concentrated in the Golgi region and in cytoplasmic vesicles. In addition MDCKII cells grown on coverslips showed a strong lateral plasma membrane staining at the sites of cell to cell contacts (Fig. 2 *d*). To visualize the spatial distribution of rab8p, fully polarized filter-grown MDCKII cells were analyzed by confocal laser beam microscopy. The digitalized data were used to generate X-Y and X-Z views of the fluorescence sequences. A focal plane along the vertical axis of MDCK taken from the upper third of the cell shows again vesicular staining and distribution of rab8p

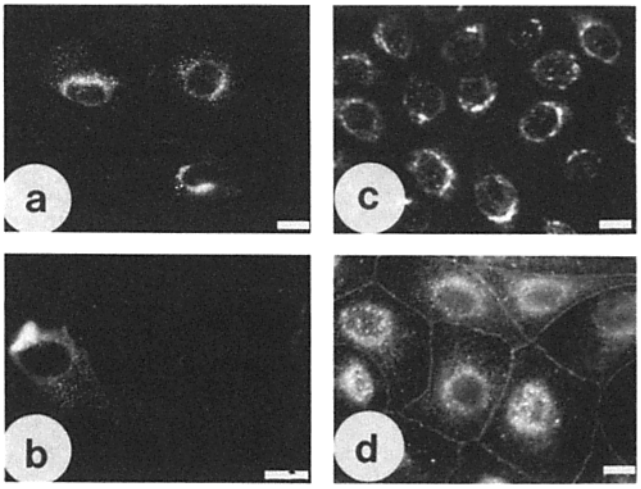

Figure 2. Immunofluorescence localization of rab8p in BHK (*a*), NIH3T3 (*b*), HeLa (*c*), and MDCKII cells (*d*). Cells were permeabilized with saponin, fixed with 3% paraformaldehyde and labeled with affinity-purified antibody against rab8p. After washing to remove unbound IgG, cells were incubated with rhodamine-labeled goat anti-rabbit IgG. Cells were viewed with a Zeiss Axiophot microscope and photographed in rhodamine optics. Antibody dilutions : (*a*) 1:25, (*b*) 1:20, (*c*) 1:80, (*d*) 1:40. Note: Since the cytoplasmic pool of rab8p was saponin extracted, the antibody specifically detects the membrane associated fraction of rab8p. Bar, 10 μm.

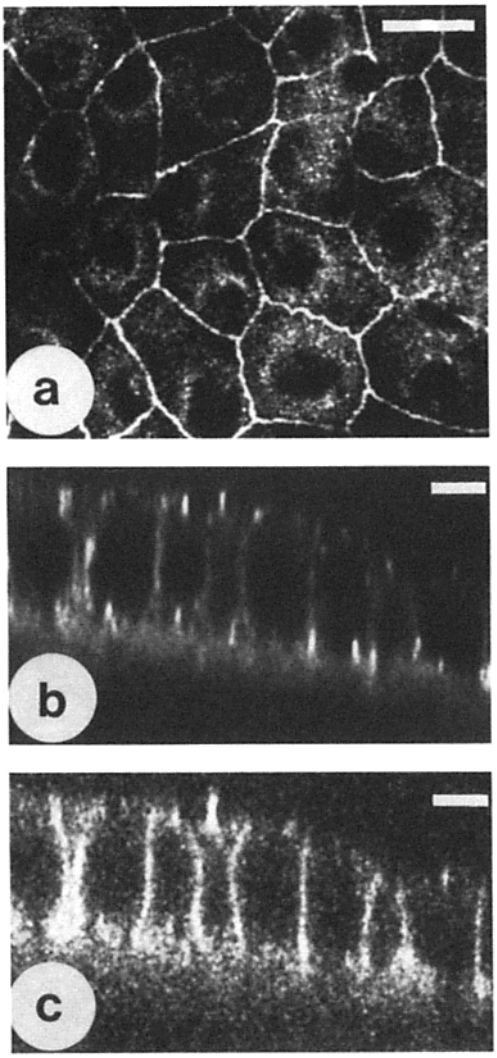

Figure. 3. Confocal laser beam immunofluorescence localization of rab8p in filter-grown MDCK II cells. Cells were grown on Transwell filters for 4 d, saponin extracted, fixed with 3% paraformaldehyde, and double labeled for indirect immunofluorescence using mAb 6.23 against the basolateral marker protein 58 kD and affinity-purified anti-rab8p antibodies. After washing to remove unbound IgG, cells were incubated with rhodamine-labeled goat anti-rabbit IgG to label the specifically bound anti-peptide rab8 IgG and with fluorescein-labeled goat anti-mouse IgG to label specifically bound 58-kD-directed antibodies. (*a*) X-Y view along the vertical axis taken from the upper third of filter-grown MDCK. Samples were photographed with rhodamine-optics showing rab8p distribution. (*b*) X-Z view of the same sample photographed with rhodamine-optics showing rab8p. (*c*) X-Z view of the same sample photographed with fluorescine optics showing 58-kD protein distribution. Bar, 10 μm.

along the basolateral plasma membrane (Fig. 3 *a*). The X-Z view (Fig. 3 *b*) confirms the basolateral localization of rab8p, but double staining with an established basolateral plasma membrane marker for MDCKII (58-kD protein; Balcarova-Ständer et al., 1984) emphasizes that rab8p is not uniformly distributed along the basolateral surface (Fig. 3 *c*). Staining was concentrated to the sites where junctional complexes are localized, and to structures at the bottom of the cell. Double staining with anti-ZO-1 antibodies (Steven-

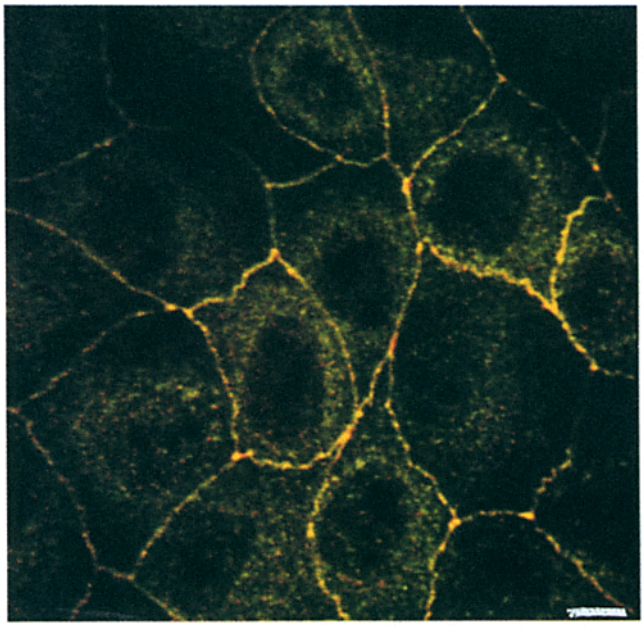

Figure 4. Confocal laser beam double-immunofluorescence localization of rab8p and ZO-1 in filter-grown MDCK II cells. Cells were grown on Transwell filters for 4 d, saponin extracted, fixed with 3% paraformaldehyde and double-labeled for indirect immunofluorescence using mAb R26 against the tight junctional protein ZO-1 and affinity-purified anti-rab8p antibodies. After washing to remove unbound IgG, cells were incubated with rhodamine-labeled goat anti-rabbit IgG to label the specifically bound anti-peptide rab8 IgG and with fluorescein-labeled goat anti-rat IgG to label specifically bound ZO-1-directed antibodies. The picture shows a X-Y overlay view along the vertical axis taken from the upper third of filter-grown MDCK. The sample was scanned with rhodamine-optics (529 nm) showing ZO-1 protein distribution in red and fluorescine optics (476 nm) showing rab8p distribution in green. Regions of overlapping distribution appear in yellow. Bar, 5 μm.

son et al., 1986) revealed a partial overlap of this marker of the tight junctions with rab8p (Fig. 4).

To extend and confirm the localization of rab8p we carried out immunoelectron microscopy on ultra thin sections of filter-grown MDCKII cells with the affinity- purified anti-peptide antibody. Specific labeling was observed on tubular and vesicular profiles close to the Golgi and on the basolateral plasma membrane (Fig. 5).

These data suggest that rab8p is associated with the Golgi region, with vesicular structures and with the basolateral plasma membrane in MDCK cells.

2D Mapping of Small GTP-binding Proteins by Expressing Full-length cDNAs with the T7 Polymerase Recombinant Vaccinia Virus System

The Reference Mapping. The vesicular staining pattern exhibited by the anti-rab8p antibody prompted us to determine whether rab8p is associated with basolateral or apical post Golgi vesicles. To this end we established a 2D gel electrophoresis mapping protocol for small GTP-binding proteins. The proteins mapped here were rab8p, rab2p, and rab10p. Overproduced rab proteins appeared as unique spots at the expected molecular weight (arrows in Fig. 6, *b–d*). In addition two unidentified GTP-binding protein spots of high intensity (Fig. 6 *a*, *A* and *B*), with apparent molecular weights of 24–25 kD, were found at identical electrophoretic positions in all cell types and most subcellular fractions studied, and served as internal positional markers.

rab8p Is Found in Immunoisolated Basolateral but not in Apical Vesicles. Basolateral and apical carrier vesicles were purified and immunoisolated as described previously (Wandinger-Ness et al., 1990). Briefly, after infection with influenza virus or with vesicular stomatitis virus and after perforation of the infected MDCKII cells we immunoisolated basolateral and apical vesicles using mAbs directed against the cytoplasmic domains of VSV-G protein and influenza virus hemagglutinin (Kreis, 1986).

The GTP-binding profiles obtained from 2D gel electrophoresis of the immunoisolated vesicle fractions are shown in Fig. 7, *a–f*. The basolateral and apical vesicles shared the same common proteins (Fig. 6, *A* and *B*), but also exhibited specific enrichment of other GTP-binding proteins. One protein (Fig. 7 *c*, *arrow*), enriched in basolateral vesicles, migrated at the position of rab8p (compare arrow in Fig. 7 *c* with arrow in Fig. 6 *c*). 2D GTP overlay experiments in MDCKII membrane fractions revealed that, like ras p21 and other small GTP-binding proteins, rab8p is of low abundance and is hardly seen in total cell extracts (Fig. 7 *a*). Therefore, the amount of rab8p in the immunoisolated basolateral vesicle fraction reflects a significant enrichment over whole membrane fractions.

Two other GTP-binding proteins were enriched in apical vesicles (Fig. 7 *e*) as compared to the vesicle preparation before immunoisolation (Fig. 7 *b*). One protein (Fig. 7 *e*, *closed arrowhead*) with an apparent molecular weight of 20–21kD (IP 3.5-4.0) could be a potential candidate for an apically enriched GTP-binding protein. However, this protein has not been identified so far by the 2D mapping. This protein is not detected in epithelial cells that have lost their apical polarity by transformation with viral k-ras (Reichmann, E., and L. A. Huber, unpublished observation), but was found in fully polarized hippocampal neurons (Dotti, C. G., and L. A. Huber, unpublished observation).

A second protein (Fig. 7 *e*, *open arrowhead*) could be rab2p or rab10p, since these proteins migrate very close to each other in the reference map (compare with Fig. 6, *b* and *d*). Neither localization nor function are known for rab10p, whereas rab2p is localized to an earlier step in the biosynthetic route (Chavrier et al., 1990*a*). The high percentage of sequence identity with SEC4/YPT1 (Chavrier et al., 1990*b*) could make rab10 a potential candidate for a post-Golgi GTP-binding protein. On the other hand a localization of rab10p to an earlier segment of the biosynthetic route, e.g., ER to Golgi cannot be ruled out at the present time. We know from recent observations that several proteins presumed to be enriched in apical vesicles are in fact known ER proteins (T. Kurzchalia, K. Fiedler, and K. Simons, unpublished observations). This contamination is probably due to the use of a temperature-sensitive mutant ts61 of the influenza virus hemagglutinin that remains in the ER at the permissive temperature because the protein is not as readily reversible after the temperature shift down, as the ts045 VSV-G protein mutant is. Therefore some ts61 hemagglutinin in the smooth ER vesicles must be carried along throughout the purification procedure and finally be immunoisolated.

These results demonstrated that rab8p is specifically as-

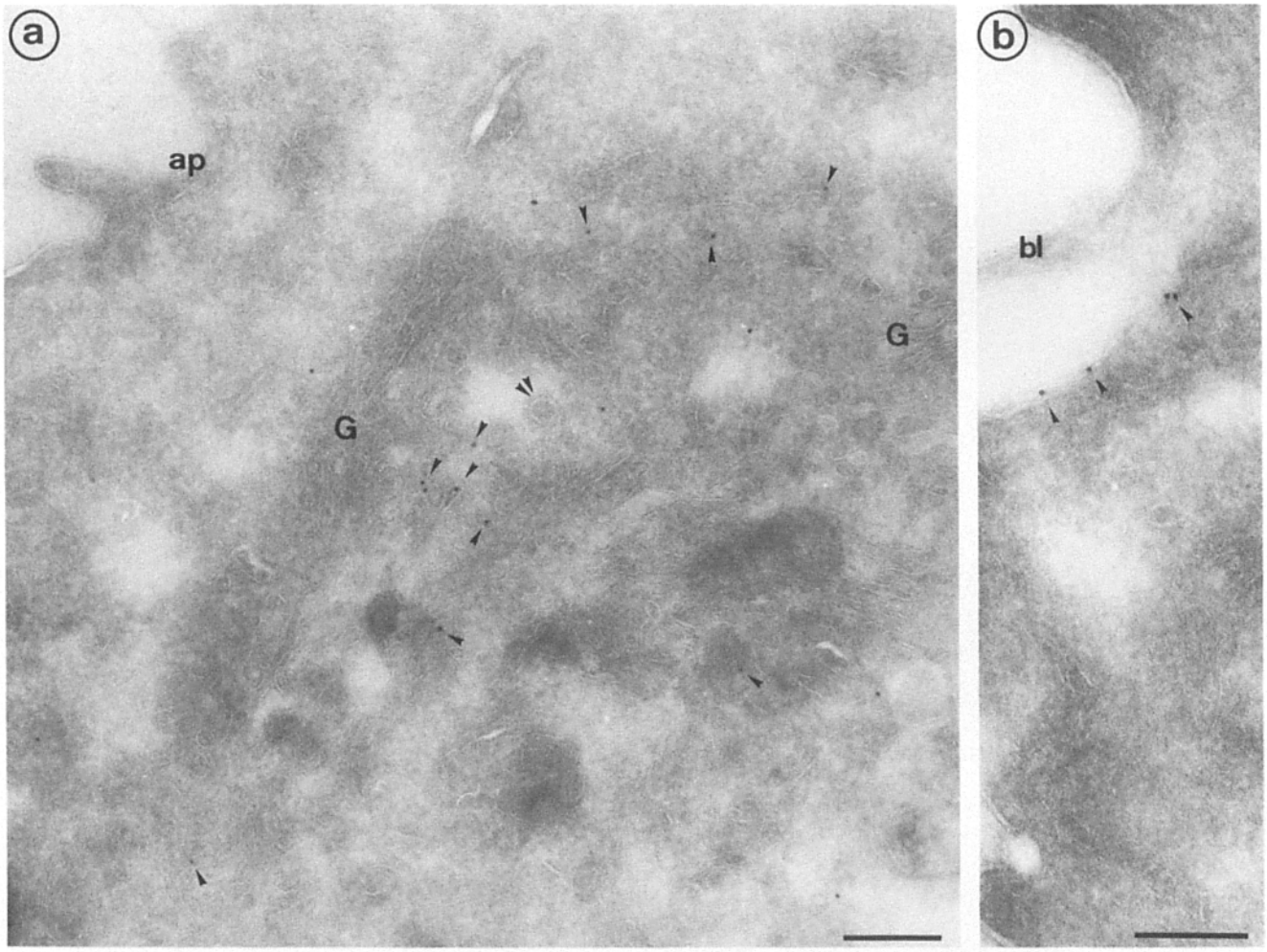

Figure 5. Immunoelectron microscopic localization of rab8p in polarized MDCK cells. Fully polarized filter-grown MDCK cells were cryosectioned perpendicular to the plane of the filter. Thawed sections were labeled with affinity-purified antibodies to rab8 followed by 9 nm protein A-gold. (*a*) Labeling for rab8 (*arrowheads*) is evident on tubular and vesicular profiles on one side of the Golgi cisternae (*G*) close to a clathrin-coated bud (*double arrowheads*). (*b*) Significant labeling is present on the cytoplasmic side of the lateral plasma membrane (*arrowheads*). No clear enrichment of rab8p in the junction region was evident by EM. Low labeling was associated with the apical surface; *bl*, basolateral plasma membrane. Bars, 200 nm.

sociated with basolateral TGN-derived vesicles. Furthermore, we identified a novel GTP-binding protein associated with apical vesicles.

ARF and β COP Are Not Present in Purified Transport Vesicles. Another subfamily of GTP-binding proteins, the ARF proteins, were enriched in the Golgi apparatus (Stearns et al., 1990) and on Golgi-derived COP-coated vesicles (Serafini et al., 1991). We tested the total fraction of flotation gradient-purified carrier vesicles (basolateral and apical) for the presence of these components using polyclonal antibodies directed against a conserved region of ARFp that recognize all mammalian ARF proteins and recombinant ARF1p (Kahn et al., 1988). TGN vesicles released from perforated cells were concentrated first by centrifugation through a sucrose cushion (Wandinger-Ness et al., 1990). This vesicle pellet is still contaminated with various membranes (ER, Golgi, plasma membrane, etc.). Western blot analysis revealed the presence of both βCOP and ARFp in this fraction (Fig. 8, lanes *1* and *3*). These membranes were then overlaid with a discontinous sucrose gradient (0.8–1.2–1.5 M) and subjected to equilibrium flotation centrifugation (Wandinger-Ness et al., 1990). The purified transport vesicles neither contained βCOP nor ARFp (Fig. 8, lanes *2* and *4*). However, since these proteins could dissociate from the vesicle membranes during isolation a possible association with TGN-derived carrier vesicles in intact cells cannot be ruled out presently.

rab8 is Functionally Involved in the Transport from TGN to the Basolateral Plasma Membrane

We next studied the involvement of rab8p in biosynthetic transport and in basolateral vs. apical post-TGN delivery. We used assays that reconstitute these processes in cells permeabilized with SLO (Kobayashi et al., 1992; Pimplikar and Simons, 1993). SLO-permeabilized, filter-grown MDCKII cells transport influenza hemagglutinin between the ER and Golgi apparatus (Kobayashi et al., 1992; Pimplikar and Simons, 1993) and deliver VSV glycoprotein and influenza hemagglutinin from the TGN to the basolateral and apical membrane domains, respectively, in a temperature, ATP and cytosol-dependent manner (Kobayashi et al., 1992; Pim-

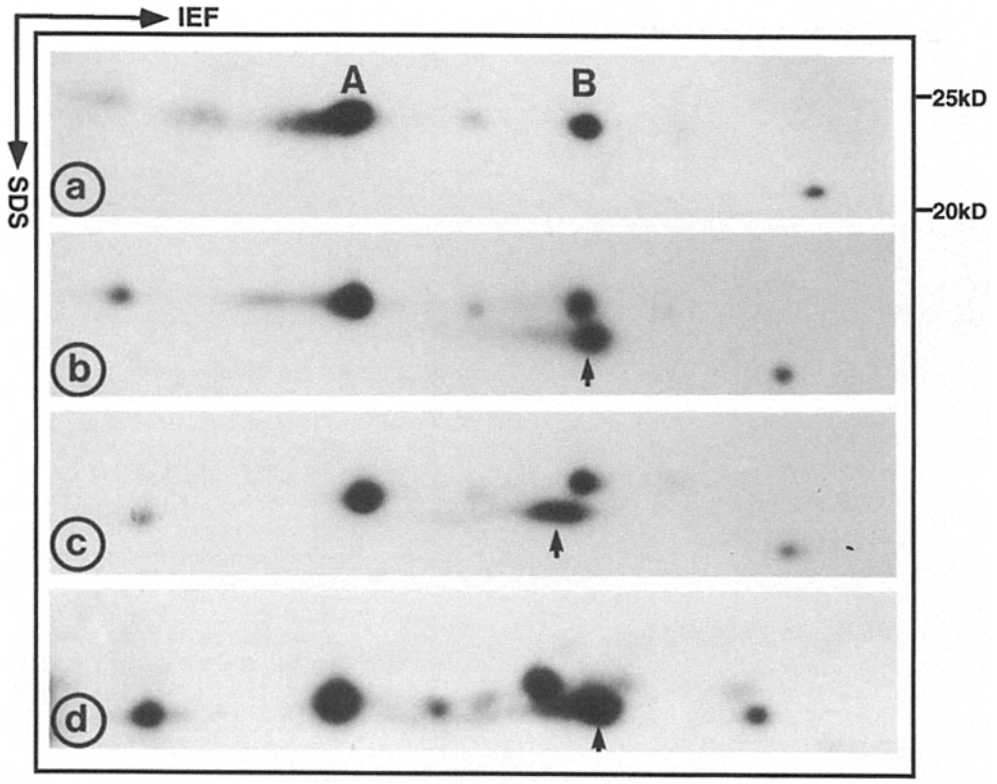

Figure 6. [α^{32}P]GTP overlay of overproduced rab proteins after high resolution 2D gel electrophoresis. Rab proteins were expressed in MDCKII cells using the T7 RNA polymerase recombinant vaccinia virus system. Microsome fractions were prepared and equal amounts of proteins (60 μg) were separated by 2D gel electrophoresis, transferred to nitrocellulose paper, and then incubated with [α^{32}P] GTP and visualized by autoradiography (12 h, −80°C). Arrows indicate overproduced rab proteins. (*a*) VT7-infected control, (*b*) VT7-rab2, (*c*) VT7-rab-8, (*d*) VT7-rab10. Proteins labeled *A* and *B* in *a* were used as internal markers with respect to their relative electrophoretic position on the blot. The area of the blot shown here represents the 20–25-kD range after 15% SDS-PAGE. The directions of IEF and SDS electrophoresis are as indicated.

plikar and Simons, 1993). To analyze the possible involvement of rab8p in these transport steps, we studied the effects of various antibodies against rab8p, or of peptides derived from the hypervariable domain at the COOH-terminus of rab8p in the permeabilized cells. The COOH-terminal hypervariable region is important for the specific localization of rab proteins (Chavrier et al., 1991) and for the interaction with the smgp25a-GDI (Araki et al., 1991). Therefore a corresponding peptide would exert an inhibitory effect by interfering with the interaction between rab proteins and factors participating in the membrane-association process. The antibodies against rab8p did not reproducibly affect any of the three transport events (data not shown). In contrast the COOH-terminal–derived peptide inhibited specifically the transport of VSV-G protein from the TGN to the basolateral plasma membrane (Fig. 9 *a*). This inhibition was concentration dependent; 50 μM of added peptide achieved 50% decrease of VSV-G transport to the basolateral surface. In contrast it did not affect either the transport of influenza–HA to the apical surface (Fig. 9 *b*) nor did it inhibit transport from the ER to the Golgi as judged by aquisition of Endo H resistance by HA (Fig. 9 *c*). Furthermore peptides derived from the NH_2-terminal region of rab5ap, that have been shown to inhibit early endosome fusion in vitro (J.-P. Gorvel, O. Steele-Mortimer, and J. Gruenberg, unpublished observation), did not affect basolateral transport (Fig. 9 *a*). These data demonstrate that a rab8 specific peptide selectively interfered with transport from the TGN to the basolateral surface.

Discussion

Rab proteins have been clearly implicated as major regulators of vesicular membrane traffic (Pfeffer, 1992; Olkkonen et al., 1993). Thus we have initiated a search for specific rab proteins involved in the delivery of vesicles to the apical and basolateral domains of polarized epithelia. This paper reports the localization of rab8p, a small GTPase highly homologous to the yeast proteins sec4p/yptlp. Immunofluorescence patterns in both polarized epithelia (MDCKII cells) and in unpolarized cells (BHK, NIH3T3, HeLa) indicated a distribution consistent with a late Golgi/plasma membrane localization of rab8p, and confirmed the widespread distribution of rab8p. Nevertheless, confocal laser beam microscopy of filter-grown, fully polarized MDCKII cells demonstrated that the protein is not distributed uniformly along the basolateral plasma membrane, but rather is enriched in areas of cell to cell contacts in close vicinity to the junctional complexes. Although the functional significance of this finding is open, the junctional complexes are highly organized and specialized membrane domains which may be involved in docking and fusion of basolateral transport vesicles, perhaps via specific receptors (c.f. Louvard, 1980). Further src kinases and levels of tyrosine phosphorylation are elevated, in adherens junctions (Tsukita et al., 1991), and specific proto-oncogenic kinases of the src family may modulate ras GAP function (for reviews see Satoh et al., 1992; Juliano and Haskill, 1993). Rab8p was also seen in restricted areas along the basal membrane. What these sites represent structurally is not yet clear.

Our immunofluorescence and immunoelectron microscopic studies gave a first clue to the site of function of rab8p along the biosynthetic route. To investigate biochemically the specific association of rab8p with transport vesicles we purified post-TGN vesicles from perforated MDCKII cells (Wandinger-Ness et al., 1990). The flotated vesicles con-

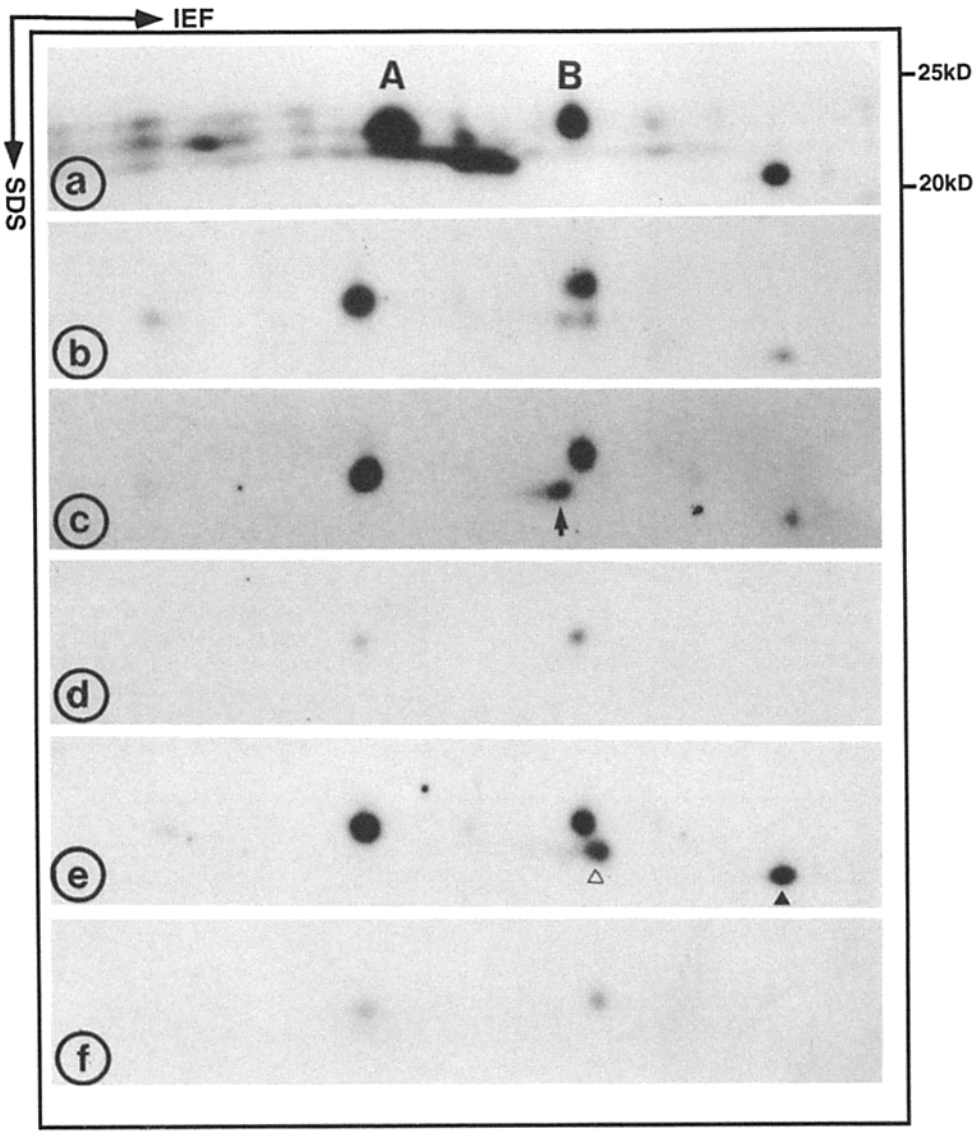

Figure 7. Analysis of small GTP-binding proteins by high resolution 2D gel electrophoresis and [α^{32}P]GTP-overlay of immunoisolated basolateral (*c*) and apical (*e*) post-TGN vesicles. A total vesicle fraction (*b*) served as starting material reference. The total membrane fraction of MDCK cells is shown in *a*. Nonspecific binding was controlled by incubating VSV containing vesicles with the antibody directed against the cytoplasmic domain of WSN HA (*d*) or by incubating HA vesicles with the antibody directed against the cytoplasmic tail of the VSV G protein (*f*). Proteins labeled with *A* and *B* in *a* were used as internal markers with respect to their relative electrophoretic position on the blot (compare to Fig. 4, *a*). Arrow in *c* indicates the specific enrichment of rab8p as compared to the expression map in Fig. 4 *c* (*arrow*). Closed and open arrow heads in *e* indicate GTP-binding proteins in the apical fraction.

tained rab8p, but neither β-COP nor ARFp, both of which are involved in vesicular transport events within the Golgi stack (Stearns et al., 1990; Serafini et al., 1991). The apical and basolateral transport vesicles from virally infected MDCK cells were immunoisolated (Wandinger-Ness et al., 1990) using the viral spike proteins as antigens. Rab8p was found to be specifically associated with basolateral vesicles. In contrast the apical vesicles were enriched in two other small GTP-binding proteins.

The ubiquitous expression of rab8 and the localization of the protein along the basolateral route points towards a regulative role in a basic membrane transport pathway present in unpolarized as well as in polarized cell types. We probed the role of rab8p in SLO-permeabilized MDCK cells to gain some insight into its possible function. SLO can be used to selectively permeabilize filter-grown MDCK cells, to analyze polarized transport of newly synthesized proteins and lipids to either the apical or to the basolateral surface domains (Gravotta et al., 1990; Kobayashi et al., 1992; Pimplikar and Simons, 1993). Drugs, peptides, or antibodies can be introduced into permeabilized cells to analyze their effects (Plutner et al., 1990). Here we could show that a synthetic peptide derived from the hypervariable COOH-terminal region of rab8p resulted in a decrease of the transport of VSV-G to the basolateral surface, but did not affect delivery of influenza HA to the apical surface nor did it inhibit ER to Golgi transport, as assayed by acquisition of Endo H resistance for HA. The strength of the SLO-permeabilized cell system is that it can be used to assay three transport events under similar conditions. This facilitates comparisons for defining specificity.

What Is the Mechanism by Which the rab8 Peptide Inhibits Transport in Vitro?

The highly variable COOH-terminal domain of rab proteins contains structural elements necessary for the association of rab proteins with their specific target membrane (Chavrier et al., 1991). It is located adjacent to the cysteine motif and should therefore lie close to the membrane. The synthetic peptide could interfere with the binding of rab8p through the COOH-terminal hypervariable region to specific receptors

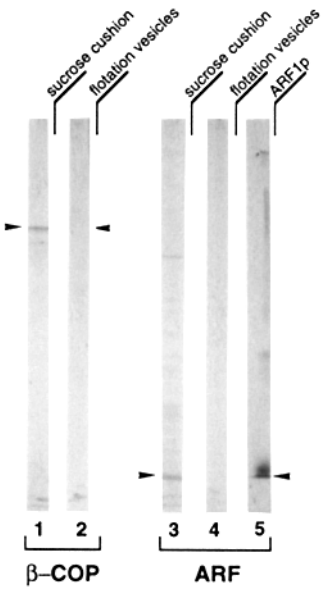

Figure 8. Immunoblot analysis of transport vesicles. The vesicle fraction budded in vitro was collected from filters of permeabilized MDCK cells (100 mm, 24 × 10^6 cells) and concentrated by centrifugation through a 0.25 M sucrose cushion (lanes *1* and *3*). This pellet was then further purified over a flotation gradient and collected at the 1.2 M–0.8 M interphase, concentrated by centrifugation, and resuspended in sample buffer (lanes *2* and *4*). Equal amounts of protein (~30 μg) were separated by preparative 10% SDS-PAGE, electrophoretically transferred onto nitrocellulose filters and strips were incubated with affinity-purified anti-ARF and affinity-purified anti-βCOP polyclonal antibodies. Bands were visualized using a HRP-conjugated secondary antibody. Lanes (*1* and *2*) anti-βCOP (1:100); lanes (*3* and *4*) anti-ARF (1:500); lane (*5*) recombinant ARFlp (50 ng). Arrowheads indicate position of proteins.

on the basolateral plasma membrane or with cytosolic proteins mediating the targeting event. In the basolateral in vitro assay system the degree of inhibition was correlated with the peptide concentration of up to 50–100 μg; a further increase in the peptide concentration did not result in further inhibition of the transport. The lack of complete inhibition could be due to several factors: first, some VSV-G on its way to the basolateral surface may already have passed the site of action of the rab8 peptides and thus could not be affected by the addition of inhibitory peptides. Second, some of the rab8 molecules could already be recruited on the membrane or in association with an interacting component and therefore this population of rab8p will be refractory to inhibitory effects of the added peptide. Finally, two different pathways between the TGN and the basolateral plasma membrane may exist, of which only one is rab8p regulated. However, the observation that the apical transport as well as ER to Golgi transport remain unaffected gives credence to our interpretation that the basolateral inhibition is a specific action of the rab8p peptide.

From these results we propose that the rab8p GTPase is a regulatory component of the basolateral transport machinery. Further work will be necessary to address the question of whether rab8 regulates vesicular budding or fusion events in TGN to basolateral transport, or rather controls the targeting of the carrier vesicles. The available tools will now make it possible to extend our investigations to other components interacting with rab8p. The function of rab8p in other

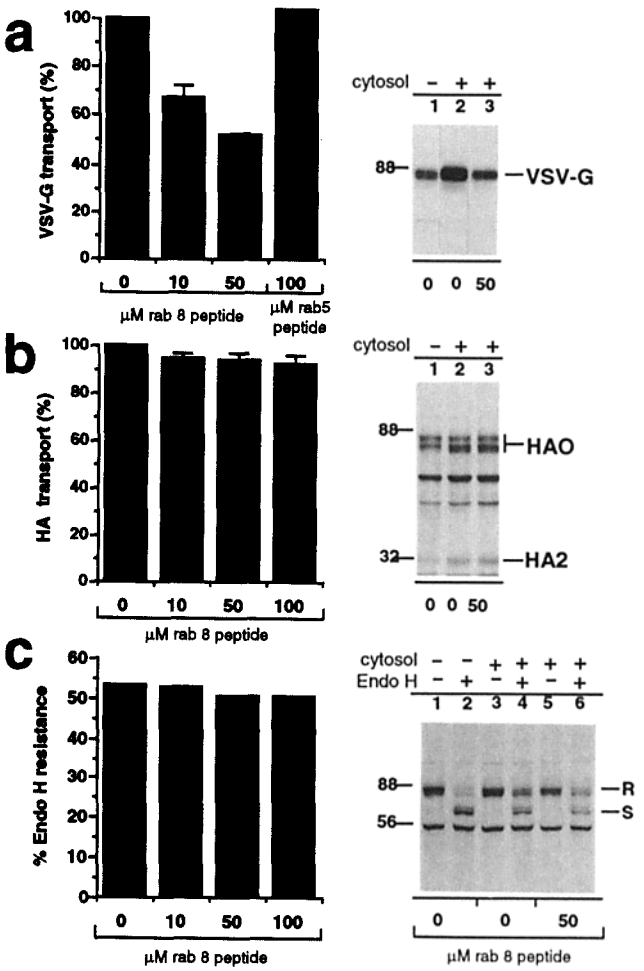

Figure 9. In vitro transport assays for rab8. Filter-grown MDCK cells were SLO permeabilized from the apical or the basolateral sides and cytosol was added back after incubation with rab8p peptides for 30 min at 4°C at the indicated concentrations. All transport experiments were performed with identical concentrations and the same batch of rab8p peptides. The dose response to peptide addition is shown in histograms. The dependence of cytosol addition and the effect of the addition of 50 μM rab8 peptides are shown in autoradiograms. All samples were analyzed by 10% SDS-PAGE, autoradiographed, scanned with a Phosphorimager (Molecular Dynamics) and the band intensities were calculated with Image Quant software. (*a*) The in vitro transport of VSV-G to the basolateral surface was performed on apically permeabilized, cytosol-depleted MDCK cells. The amount of VSV-G protein transported to the basolateral surface was calculated as the amount of VSV-G bound to protein A-agarose after surface immunoprecipitation with G-specific antibodies. The histogram shows cytosol dependent transport as being 100% (transport in the presence of cytosol − transport in the absence of added cytosol). Values are means ± standard errors from four experiments performed with duplicate filters. The last bar in the histogram shows a representative experiment with the NH_2-terminal rab5a peptide. (*b*) The in vitro transport of influenza HA to the apical surface was performed on basolaterally permeabilized and cytosol depleted MDCK cells. Arrival of HA at the apical plasma membrane was measured by its sensitivity to cleavage of trypsin. The values are expressed as cytosol dependent transport being 100%. Values are means ± standard errors from three experiments performed with duplicate filters (% transport = 2 × HA2/HA0 + HA2 × 100). (*c*) The in vitro transport of HA from ER to Golgi was performed on basolaterally permeabilized and cytosol-depleted MDCK cells. The cell lysates were either treated with 66 mM Na-citrate buffer, pH 5, alone or with 50 mU Endo H in the above buffer at 37°C for 20 h. *R*, Endo H–resistant form; *S* Endo H–sensitive form. Values in the histogram represent means of Endo H resistance for HA in percent from duplicate filters (HA resistant/HA resistant + HA sensitive).

cell types will also have to be studied, and the accompanying paper (Huber et al., 1993) shows that rab8p functions in the delivery of viral glycoproteins to the dendrites of polarized hippocampal neurons.

We would like to thank Dr. E. Ikonen for her support and help with the in vitro transport experiments and C. Frederiksen for technical assistance. We would also like to thank Dr. S. Pfeiffer for helpful discussions and critically reading the manuscript. We are particular grateful to Dr. P. Dupree for providing *E. coli* expressed rab proteins and to Drs. R. Kahn and T. Kreis for generous gifts of antibodies. The transwell filters were a kind gift from Hank Lane, Costar Corp. (Cambridge, MA).

L. A. Huber was a recipient of the Erwin Schrödinger-fellowship from the Austrian ministry of sciences. We were supported by SFB 352 from Deutsche Forschungs Gemeinschaft (DFG).

Received for publication 4 March 1993 and in revised form 17 June 1993.

References

Araki, S., K. Kaibuchi, T. Sasaki, Y. Hata, and Y. Takai. 1991. Role of the C-terminal region of smgp25a in its interaction with membranes and the GDP/GTP exchange protein. *Mol. Cell. Biol.* 11:1438–1447.

Bacallao, R., C. Antony, C. Dotti, E. Karsenti, E. H. K. Stelzer, and K. Simons. 1989. The subcellular organization of Madin-Darby Canine kidney cells during the formation of a polarized epithelium. *J. Cell Biol.* 109:2817–2832.

Balcarova-Ständer, J., S. E. Pfeiffer, S. E. Fuller, and K. Simons. 1984. Development of cell surface polarity in the epithelial Madin-darby canine kidney (MDCK) cell line. *EMBO (Eur. Mol. Biol. Organ.) J.* 3:2687-2694.

Balch, W. E. 1990. Small GTP-binding proteins in vesicular transport. *Trends Biochem. Sci.* 15:473–477.

Bennett, M. K., A. Wandinger-Ness, and K. Simons. 1988. Release of putative exocytic transport vesicles from perforated MDCK cells. *EMBO (Eur. Mol. Biol. Organ.) J.* 7:4075–4085.

Bourne, H. R. 1988. Do GTPases direct membrane traffic in secretion. *Cell.* 53:669–671.

Bravo, R. 1984. Two-dimensional gel electrophoresis: A guide for the beginner. *In* Two-dimensional Gel Electrophoresis of Proteins. J.E. Celis and R. Bravo, editors. Academic Press, Orlando, FL. 3–36.

Bucci, C., R. Frunzio, L. Schiariotti, A. L. Brown, M. M. Rechler, and C. B. Bruni. 1988. A new member of the ras gene superfamily identified in a rat liver cell line. *Nucleic Acids Res.* 16:9979–9993.

Bucci, C., R. G. Parton, I. H. Mather, H. Stunnenberg, K. Simons, B. Hoflack, and M. Zerial. 1992. The small GTPase rab5 functions as a reg-ulatory factor in the early endocytic pathway. *Cell.* 70:715–728.

Burstein, E. S., K. Linko-Stentz, Z. Lu, and I. G. Macara. 1991. Regulation of the GTPase activity of the *ras*-like protein $p25^{rab3A}$. Evidence for a *rab3A*-specific GAP. *J. Biol. Chem.* 266:2689–2692.

Celis, J. E., B. Gesser, H. H. Rasmussen, P. Madsen, H. Leffers, K. Dejgaard, B. Honoré, E. Olsen, G. Ratz, J. B. Lauridsen, B. Basse, S. Mouritzen, M. Hellerup, A. Andersen, E. Walbum, A. Celis, G. Bauw, M. Puype, J. Van Damme, and J. Vandekerckhove. 1990. Comprehensive 2 D gel protein databases offer a global approach to the analysis of human cells: the transformed amnion cells (AMA) master database and its link to genome DNA sequence data. *Electroph.* 11:989–1071.

Chardin, P. and A. Tavitian. 1989. The ral gene: a new ras related gene isolated by the use of a synthetic probe. *EMBO (Eur. Mol. Biol. Organ.) J.* 8:2203-2208.

Chardin, P., P. Madaule, and A. Tavitian. 1988. Coding sequence of human rho cDNAs clone 6 and clone 9. *Nucleic Acids Res.* 16:2717.

Chavrier, P., R. G. Parton, H. P. Hauri, K. Simons, and M. Zerial. 1990*a*. Localization of low molecular weight GTP binding proteins to exocytic and endocytic compartments. *Cell.* 62:317–329.

Chavrier, P., M. Vingron, C. Sander, K. Simons, and M. Zerial. 1990*b*. Molecular cloning of YPT1/SEC4-related cDNAs from an epithelial cell line. *Mol. Cell. Biol.* 10:6578–6585.

Chavrier, P., J.-P. Gorvel, E. Stelzer, K. Simons, J. Gruenberg, and M. Zerial. 1991. Hypervariable C-terminal domain of rab proteins acts as a targeting signal. *Nature (Lond.).* 353:769–772.

Chavrier, P., K. Simons, and M. Zerial. 1992. The complexity of the Rab and Rho GTP-binding protein subfamilies revealed by a PCR cloning approach. *Gene.* 112:261–264.

Darchen, F., A. Zahraoui, F. Hammel, M.-P. Monteils, A. Tavitian, and D. Scherman. 1990. Association of the GTP-binding protein Rab3A with bovine adrenal chromaffin granules. *Proc. Natl. Acad. Sci. USA.* 87: 5692–5696.

Didsbury, J., R. F. Weber, G. M. Bokoch, T. Evans, and R. Snyderman, 1989. rac, a novel ras-related family of proteins that are Botulinum Toxin substrates. *J. Biol. Chem.* 264:16378–16382.

Fischer von Mollard, G., T. C. Südhof, and R. Jahn. 1991. A small GTP-binding protein dissociates from synaptic vesicles during exocytosis. *Nature (Lond.).* 349:79–81.

Fuerst, T. R., E. G. Niles, F. W. Studier, and B. Moss. 1986. Eukaryotic transient-expresion system based on recombinant vaccinia virus that synthesizes bacteriophage T7 RNA polymerase. *Proc. Natl. Acad. Sci. USA.* 83:8122–8126.

Gallwitz, D., C. Donath, and C. Sander. 1983. A yeast gene encoding a protein homologous to the human c-has/bas proto-oncogene product. *Nature (Lond.).* 306:704–707.

Gorvel, J.-P., P. Chavrier, M. Zerial, and J. Gruenberg. 1991. rab5 controls early endosome fusion in vitro. *Cell.* 64:915–925.

Goud, B., A. Zahraoui, A. Tavitian, and J. Saraste. 1990. Small GTP-binding protein associated with Golgi cisternae. *Nature (Lond.).* 345:553–556.

Gravotta, D., M. Adesnik, and D. D. Sabatini. 1990. Transport of influenza HA from the trans-Golgi network to the apical surface of MDCK cells permeabilized in their basolateral plasma membranes: Energy dependence and involvement of GTP-binding proteins. *J. Cell Biol.* 111:2893–2908.

Griffiths, G. and K. Simons. 1986. The trans golgi network: sorting at the exit of the golgi complex. *Science (Wash. DC).* 234:438–443.

Griffiths, G., A. McDowall, R. Back, and J. Dubochet. 1984. On the preparation of cryosections for immunocytochemistry. *J. Ultrastruct. Res.* 89: 65–78.

Griffiths, G., S. Pfeiffer, K. Simons, and K. Matlin. 1985. Exit of newly synthesized membrane proteins form the trans cisternae of the Golgi complex to the plasma membrane. *J. Biol. Chem.* 101:949–964.

Hall, A. 1991. GTP-binding proteins. *Curr. Opin. Cell Biol.* 1:817–820.

Huber, L.A., M. J. de Hoop, P. Dupree, M. Zerial, K. Simons, and C. Dotti. 1993. Protein transport to the dendritic plasma membrane of cultured neurons is regulated by rab8p. *J. Cell Biol.* 123:47–55.

Hughson, E., A. Wandinger-Ness, H. Gausepohl, G. Griffiths, and K. Simons. 1988. The cell biolog of enveloped virus infection of epithelial tissues. In The molecular biology of infectious diseases. Centenary Symposium of the Pasteur Institute. M. Schwartz, editor. (Elsevier Press, Paris) 75–89.

Juliano, R.L. and S. Haskill. 1993. Signal transduction from the extracellular matrix. *J. Cell Biol.* 120:577–585.

Kahn, R. A., C. Goddard, and M. Newkirk. 1988. Chemical and immunological characterization of the 21-kDa ADP-ribosylation factor of adenylate cyclase. *J. Biol. Chem.* 263:8282–8287.

Kahn, R. A., P. Randazzo, T. Serafini, O. Weiss, C. Rulka, J. Clark, M. Amherdt, P. Roller, L. Orci, and J. E. Rothman. 1992. The amino terminus of ADP-ribosylation factor (ARF) is a critical determinant of ARF activities and is a potent and specific inhibitor of protein transport. *J. Biol. Chem.* 267:13039–13046.

Kobayashi, T., S. W. Pimplikar, R. G. Parton, S. Bhakdi, and K. Simons. 1992. Sphingolipid transport from the trans-Golgi network to the apical surface in permeabilized MDCK cells. *FEBS (Fed. Eur. Biochem. Soc.) Lett.* 300:227–231.

Koch, G., B. Habermann, C. Mohr, I. Just, and K. Aktories. 1992. ADP-ribosylation of rho proteins is inhibited by melittin, mast cell degranulating peptide and compound 48/80. *Eur. J. Pharmacol. Mol. Pharmacol.* 226: 87–91.

Kreis, T. E., 1986. Microinjected antibodies against the cytoplasmic domain of vesicular stomatitis virus glycoprotein block its transport to the cell surface. *EMBO (Eur. Mol. Biol. Organ.) J.* 5:931–941.

Kurzchalia, T. V., P. Dupree, R. G. Parton, R. Kellner, H. Virta, M. Lehnert, and K. Simons. 1992. VIP21, a 21-kD membrane protein is an integral component of *trans*-Golgi-network-derived transport vesicles. *J. Cell Biol.* 118:1003–1014.

Lapetina, E. and B. Reep. 1987. Specific binding [alpha 32P]GTP to cytosolic and membrane-bound proteins of human platelets correlates with the activation of phospholipase C. *Proc. Natl. Acad. Sci. USA.* 84:2261–2265.

Lenhard, J. M., R. A. Kahn and P. D. Stahl. 1992. Evidence for ADP-ribosylation factor (ARF) as a regulator of *in vitro* endosome-endosome fusion. *J. Biol. Chem.* 267:13047–13052.

Lombardi, D., T. Soldati, M. A. Riederer, Y. Goda, M. Zerial, and S. R. Pfeffer. 1993. Rab9 functions in transport between late endosomes and the trans Golgi network. *EMBO (Eur. Mol. Biol. Organ.) J.* 12:677–682.

Louvard, D. 1980. Apical membrane aminopeptidase appears at site of cell-cell contact in cultured kidney epithelial cells. *Proc. Natl. Acad. Sci. USA.* 77:4132–4136.

Matlin, K. S., and K. Simons. 1984. Sorting of an apical plasma membrane glycoprotein occurs before it reaches the cell surface in cultured epithelial cells. *J. Cell Biol.* 99:2131–2139.

Matlin, K. S., H. Reggio, A. Helenius, and K. Simons. 1981. Infectious entry pathway of influenza virus in a canine kidney cell line. *J. Cell Biol.* 91:601–613.

Mizoguchi, A., S. Kim, T. Ueda, and Y. Takai. 1989. Tissue distribution of smg p25A, a ras p21-like GTP-binding protein, studied by use of a specific monoclonal antibody. *Biochem. Biophys. Res. Commun.* 162:1438–1445.

Oka, T., S. Nishikawa, and A. Nakano. 1991. Reconstitution of GTP-binding Sar1 protein function in ER to Golgi transport. *J. Cell Biol.* 114, 671–679.

Olkkonen, V.M., P. Dupree, L. A. Huber, A. Lütcke, M. Zerial, and K. Simons. 1993. Compartmentalization of rab proteins in mammalian cells. In GTPases in Cell Biology. B. Dickey and L. Birnbaumer, editors. Springer

Verlag. Heidelberg. In press.
Pfeffer, S. R. 1992. GTP-binding proteins in intracellular tranport. *Trends Cell Biol.* 2:41–46.
Pfeiffer, S., S. D. Fuller, and K. Simons. 1985. Intracellular sorting and basolateral appearance of the G protein of vesicular stomatitis virus in Madin-Darby canine kidney cells. *J. Cell Biol.* 101, 470–476.
Pimplikar, S. W., and K. Simons. 1993. Apical transport in epithelial cells is regulated by a Gs class of heterotrimeric G protein. *Nature (Lond.).* 362:456–458.
Pizon, V., P. Chardin, I. Lerosey, B. Olofsson, and A. Tavitian. 1988. Human cDNAs rap1 and rap2 homologous to the Drosophila gene Dras3 encode proteins closely related to ras in the 'effector' region. *Oncogene.* 3:201–204.
Plutner, H., R. Schwaninger, S. Pind, and W. E. Balch. 1990. Synthetic peptides of the rab effector domain inhibit vesicular transport through the secretory pathway. *EMBO (Eur. Mol. Biol. Organ.) J.* 9:2375–2383.
Polakis, P. G., R. F. Weber, B. Nevins, J. R. Didsbury, T. Evans, and R. Snyderman. 1989. Identification of the ral and racl gene products, low molecular mass GTP-binding proteins from human platelets. *J. Biol. Chem.* 264:16383–16389.
Salminen, A. and P. J. Novick. 1987. A ras-like protein is required for a post-golgi event in yeast secretion. *Cell.* 49:527–538.
Sasaki, T., K. Kaibuchi, A. K. Kabcenell, P. J. Novick, and Y. Takai. 1991. A mammalian inhibitory GDP/GTP exchange protein (GDP dissociation inhibitor) for *smg* p25A is active on the yeast *SEC4* protein. *Mol. Cell. Biol.* 11:2909–2912.
Satoh, T., M. Nakafuku, and Y. Kaziro. 1992. Function of Ras as a molecular switch in signal transduction. *J. Biol. Chem.* 267:24149–24152.
Segev, N., J. Mulholland, and D. Botstein. 1988. The yeast GTP-binding YPT1 protein and a mammalian counterpart are associated with the secretion machinery. *Cell* 52:915–924.
Serafini, T., L. Orci, M. Amherdt, M. Brunner, R. A. Kahn, and J. E. Rothman. 1991. ADP-ribosylation factor is a subunit of the coat of Golgi-derived COP-coated vesicles: A novel role for a GTP-binding protein. *Cell* 67:239–253.
Sewell, J. L., and R. A. Kahn. 1988. Sequences of the bovine and yeast ADP-ribosylation factor and comparison to other GTP-binding proteins. *Proc. Natl. Acad. Sci. USA.* 85:4620–4624.
Shimizu, K., K. Kaibuchi, H. Nonaka, J. Yamamoto, and Y. Takai. 1991. Tissue and subcellular distributions of an inhibitory GDP/GTP exchange protein (GDI) for the *rho* proteins by use of its specific antibody. *Biochem. Biophys. Res. Commun.* 175:199–206.
Stearns, T., M. C. Willingham, D. Botstein, and R. A. Kahn. 1990. ADP-ribosylation factor is functionally and physically associated with the Golgi complex. *Proc. Natl. Acad. Sci. USA* 87:1238–1242.
Stevenson, B. R., J. D. Siliciano, M. S. Moosekev, and D. A. Goodenough. 1986. Identification of ZO-1: a high molecular weight polypeptide associated with the tight junction (zonula occludens) in a variety of epithelia. *J. Cell Biol.* 103:755–766.
Studier, F. W., A. H. Rosenberg, J. J. Dunn, and J. W. Dubendorff. 1990. Use of T7 RNA polymerase to direct expression of cloned genes. *Methods Enzymol.* 185:60–89.
Tan, T. J., P. Vollmer, and D. Gallwitz. 1991. Identification and partial purification of GTPase-activating proteins from yeast and mammalian cells that preferentially act on Ypt1/Rab1 proteins. *FEBS (Fed. Eur. Biochem. Soc.) Lett.* 291:322–326.
Touchot, N., P. Chardin, and A. Tavitian. 1987. Four additional members of the ras gene superfamily isolated by oligonucleotide strategy: molecular cloning of YPT-related cDNA from a rat brain library. *Proc. Natl. Acad. Sci. USA.* 84:8210–8214.
Tsukita, S., K. Oishi, T. Akiyama, Y. Yamanashi, and T. Yamamoto. 1991. Specific proto-oncogenic tyrosine kinases of src family are enriched in cell-to-cell adherens junctions where the level of tyrosine phosphorylation is elevated. *J. Cell Biol.* 113:867–879.
Van der Sluijs, P., M. Hull, A. Zahraoui, A. Tavitian, B. Goud, and I. Mellman. 1991. The small GTP-binding protein rab4 is associated with early endosomes. *Proc. Natl. Acad. Sci. USA.* 88:6313–6317.
Van der Sluijs, P., M. Hull, L. A. Huber, P. Male, B. Goud, and I. Mellman. 1992. Reversible phosphorylation-dephosphorylation determines the localization of rab4 during cell cycle. *EMBO (Eur. Mol. Biol. Organ.) J.* 11: 4379–4389.
Wandinger-Ness, A., M. K. Bennett, C. Antony, and K. Simons. 1990. Distinct transport vesicles mediate the delivery of plasma membrane proteins to the apical and basolateral domains of MDCK cells. *J. Cell Biol.* 111:987–1000.
Zahraoui, A., N. Touchot, P. Chardin, and A. Tavitian. 1988. Complete coding sequences of the ras related rab 3 and 4 cDNAs. *Nucleic Acids Res.* 16:1204.
Zahraoui, A., N. Touchot, P. Chardin, and A. Tavitian. 1989. The human rab genes encode a family of GTP binding proteins related to yeast YPT1 and SEC4 products involved in secretion. *J. Biol. Chem.* 264:12394–12401.